Nanoscale

PAPER

View Article Online
View Journal | View Issue

Cite this: *Nanoscale*, 2014, **6**, 2146

Transport of nanoparticles through the blood–brain barrier for imaging and therapeutic applications

Malka Shilo, Menachem Motiei, Panet Hana and Rachela Popovtzer*

A critical problem in the treatment of neurodegenerative disorders and diseases, such as Alzheimer's and Parkinson's, is the incapability to overcome the restrictive mechanism of the blood–brain barrier (BBB) and to deliver important therapeutic agents to the brain. During the last decade, nanoparticles have gained attention as promising drug delivery agents that can transport across the BBB and increase the uptake of appropriate drugs in the brain. In this study we have developed insulin-targeted gold nanoparticles (INS-GNPs) and investigated quantitatively the amount of INS-GNPs that cross the BBB by the receptor-mediated endocytosis process. For this purpose, INS-GNPs and control GNPs were injected into the tail vein of male BALB/c mice. Major organs were then extracted and a blood sample was taken from the mice, and thereafter analyzed for gold content by flame atomic absorption spectroscopy. Results show that two hours post-intravenous injection, the amount of INS-GNPs found in mouse brains is over 5 times greater than that of the control, untargeted GNPs. Results of further experimentation on a rat model show that INS-GNPs can also serve as CT contrast agents to highlight specific brain regions in which they accumulate. Due to the fact that they can overcome the restrictive mechanism of the BBB, this approach could be a potentially valuable tool, helping to confront the great challenge of delivering important imaging and therapeutic agents to the brain for detection and treatment of neurodegenerative disorders and diseases.

Received 12th September 2013
Accepted 24th November 2013

DOI: 10.1039/c3nr04878k

www.rsc.org/nanoscale

Introduction

A critical problem in the treatment of neurodegenerative disorders and diseases, such as Alzheimer's and Parkinson's, is the incapability to overcome the restrictive mechanism of the blood–brain barrier (BBB) and to deliver important therapeutic agents to the brain.[1–3] The BBB is the major interface between the blood and the brain, protecting it from harmful blood-borne substances, microorganisms, hormones and neurotransmitters, and maintaining central nervous system (CNS) homeostasis. Although specific and selective transporters located on the BBB supply the CNS with glucose, free fatty acids, amino acids, vitamins, minerals, and electrolytes,[4] nearly all high molecular weight drugs and more than 98% of low molecular weight drugs cannot cross the BBB.[5]

During the last decade, nanoparticles have gained attention as promising drug delivery agents that can transport across the BBB and increase the uptake of appropriate drugs in the brain.[3,6–9] The important advantages of nanoparticle–drug complexes over the NP-free drug are due mainly to prolonged blood circulation, controlled biodistribution and specific molecular targeting capabilities.[10–13] In contrast to the delivery of nanoparticles to tumors that usually occurs through the "leaky" tumor vasculature,[14,15] which is known as the enhanced permeability and retention (EPR) effect, the delivery of the nanoparticles to the brain is mainly based on the prolonged blood circulation time. Increasing the duration of drug circulation in the blood facilitates the drug's ability ability to interact with specific transporters and/or receptors expressed on the luminal side of BBB endothelial cells, and consequently to cross the BBB. Among the few possible BBB penetration routes, receptor-mediated endocytosis has been shown to be the most efficient transport mechanism, especially for large molecules, proteins and nanoparticles.[3,14] Such receptor-mediated transport employs the vesicular trafficking system of the brain endothelium to transport substances such as insulin, transferrin, low density lipoprotein, lactoferrin and other peptides across the BBB.[16–18] Receptor-mediated endocytosis takes place at the luminal (blood) side, after which the compound moves through the cytoplasm of the endothelial cell, and is finally exocytosed into the brain capillary endothelium[16,18,19] (Fig. 1). Previous studies have demonstrated efficient drug transport across the BBB by covalent attachment of apolipoprotein A1, B, or E, transferrin or antitransferrin antibodies to the nanoparticles.[20–23]

Recently, Ulbrich *et al.* qualitatively demonstrated that targeting the insulin receptor is an attractive strategy for efficient drug delivery into the brain because insulin receptors have been

Bar-Ilan University, Faculty of Engineering & Institute of Nanotechnology & Advanced Materials, Ramat Gan 52900, Israel. E-mail: rachela.popovtzer@biu.ac.il

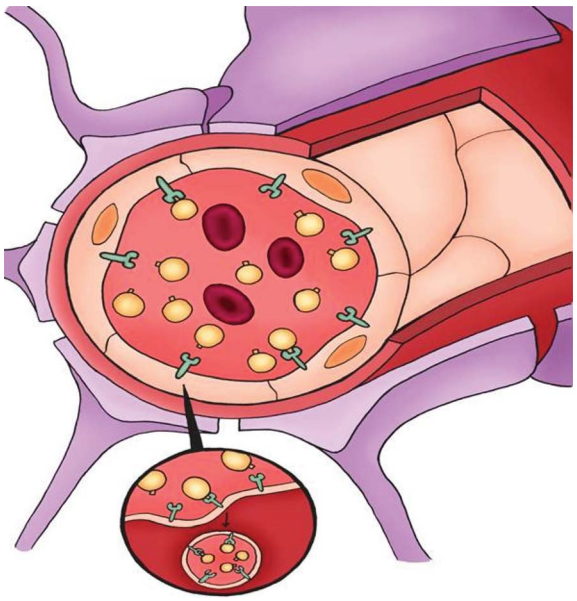

Fig. 1 Schematic presentation of targeted delivery of INS-GNPs across the BBB *via* receptor-mediated endocytosis. Cerebral blood vessel contains GNPs (yellow) that are covalently coated with insulin (small knobs, dark yellow), and insulin receptors (green) that expressed on the luminal side of BBB endothelial cells. The INS-GNPs are coupled to the insulin receptors and cross the BBB *via* receptor-mediated endocytosis (shown in the small circle).

shown to be 10 times more effective than transferrin receptors, in traversing the BBB.[23] Intravenous injection of loperamide-loaded human serum albumin nanoparticles with covalently bound insulin or 29B4 antibodies induced significant antinociceptive effects in a tail-flick test in ICR (CD-1) mice, demonstrating that insulin-targeted nanoparticles are able to target the insulin receptors on the BBB and to transport a drug into the brain. This study also proved that the passage of these nanoparticles is mediated by insulin receptors, as pre-injection of anti-insulin receptor–antibody totally inhibited the delivery of loperamide.[23]

Quantitative investigation of the amount of INS-GNPs that cross the BBB, the main goal of the present study, is essential for determining the potential therapeutic effect of this approach. In addition, beyond the ability of the INS-GNPs to act as a drug carrier, the delivery of insulin into the brain could potentially be a new therapy approach for patients with Alzheimer's disease. Insulin receptors, which are present in high levels in several regions within the brain, such as the hypothalamus, hippocampus and cerebral cortex,[19,24] modulate the levels of β-amyloid peptides and protect against the harmful effects of these peptides on the synapses.[25]

Previous studies revealed a correlation between the amount of insulin in the brain and Alzheimer's disease.[25–27] It has been demonstrated that individuals with Alzheimer's disease have reduced brain insulin receptor expression and therefore lower cerebrospinal fluid insulin levels. Administration of insulin to these patients improved their memory and performance, establishing that restoring the insulin in the brain to normal levels may provide therapeutic benefit in Alzheimer's disease.[25,28] However, since delivery of endogenous insulin causes glucose imbalance, rendering it unfeasible, an alternative strategy is suggested by conjugating insulin to nanoparticles. Glucose imbalance does not occur with the use of INS-GNPs because nanoparticle distribution is limited to organs within the lymphatic and excretory systems, and to pathologies associated with increased angiogenic conditions. While high levels of insulin receptors can be found in other organs, such as the parenchymal cells in the heart, skeletal muscle and fat tissues, capillaries that perfuse these organs have continuous endothelial barriers which impede significant entry of nanoparticles from circulation into the organ interstitium,[1,19,29] and thus, unlike endogenous insulin, insulin-linked nanoparticles cannot enter these organs. In contrast, insulin receptors found on the luminal membrane of brain capillary endothelial cells can cause a receptor-mediated endocytosis process across the BBB. By delivering a sufficient amount of insulin to the brain without affecting glucose balance, these nanoparticles can serve as efficient drug delivery carriers.

In this study we show a quantitative investigation on the amount of INS-GNPs that cross the BBB, as well as their biodistribution and pharmacokinetics for 48 hours. In addition to the potential use of INS-GNPs as a drug treatment (insulin) or as drug carriers (by conjugating different drugs to the particles), nanoparticles made out of gold demonstrate their potential as CT imaging contrast agents.

Experimental

GNPs have been chosen as a model system since they have several important advantages. They have a high degree of flexibility in terms of particle size, shape and functional groups for coating and targeting. Their potential for clinical implementation has led to substantial research regarding their *in vivo* chemical stability,[10,30,31] pharmacokinetics,[10] biodistribution[31–36] and bio-toxicity.[10,32,37–40] They are well known for their biosafety and have been shown to have long circulation times.[41–45] Most importantly, GNPs can be quantitatively detected in the brain by atomic absorption methods (*ex vivo*), and detected *in vivo* by CT imaging, as they are ideal CT contrast agents. Due to its high atomic number, gold induces strong X-ray attenuation which can differentiate targeted tissue from surrounding non-targeted tissue.[46]

Chemicals

Hydrogen tetrachloroaurate(III) trihydrate (HAuCl4) was purchased from Strem, USA. Heterofunctional polyethylene glycol (PEG), methoxy-PEG-SH (mPEG-SH $M_w \sim 5.0$ kDa) and carboxylic acid-PEG-SH (SH-PEG–COOH $M_w \sim 3.4$ kDa) were purchased from Creative PEGWorks, Winston Salem, NC, USA. Human Insulin was purchased from Novo Nordisk A/S, Denmark. 1-Ethyl-3-(3-dimethylaminopropyl) carbodiimide HCl (EDC) and *N*-hydroxysulfosuccinimide sodium salt (NHS) were purchased from Thermo Scientific, USA.

GNP synthesis and conjugation

GNPs were prepared using sodium citrate according to the known methodology described by Enüstun and Turkevich.[47] In this method 520 μl 50% w/v of $HAuCl_4$ mixed with 200 ml purified water was used. This mixture was heated until boiling, and then 4.04 ml sodium citrate was added. Ten minutes later, the solution was removed from the plate and left for refrigeration. The solution was centrifuged until precipitation of nanoparticles and a clear suspension is obtained.

For insulin receptor targeting, GNPs were coated with a layer of PEG that composed of a mixture of mPEG-SH (85%) and SH-PEG–COOH (15%) (Fig. 2a). The PEG layer was covalently conjugated to insulin (400 μl, insulin human, 100 IU ml^{-1}, Novo Nordisk A/S, Denmark) by addition of EDC and NHS (200 μl of each chemical, Thermo Scientific, USA) to the solution. The solution was left to stir overnight in order to ensure the conjugation of the PEG layer to the insulin. The INS-GNPs were purified after the solution was centrifuged until obtaining a clear suspension. The final concentration of the INS-GNPs was 30 mg ml^{-1}. For control nanoparticles, GNPs were coated with mPEG-SH. The control nanoparticles were purified in the same manner as the INS-GNPs until reaching a final concentration of 30 mg ml^{-1}.

GNP characterization

The size, shape and uniformity of the GNPs were measured using transmission electron microscopy (TEM) (JEM-1400, JEOL). Samples were prepared by drop-casting 5 μl of the GNP solution onto a standard carbon-coated film on a cooper grid. Samples were left to dry in a vacuum desiccator until the TEM experiment. The GNPs were further characterized using ultraviolet-visible spectroscopy (UV-1650 PC; Shimadzu Corporation, Kyoto Japan) following each level of coating.

Animal model and *in vivo* experiments

Male BALB/c mice, each weighing 20–25 g, were divided into two groups for use in *in vivo* experiments. The first group was injected with 200 μl of 30 mg ml^{-1} INS-GNPs into the tail vein. The mice were anesthetized and sacrificed at 0.5, 2, 24 and 48 hours post-injection (in each experiment, three mice were used for each time point after the injection). The second group was injected with 200 μl of 30 mg ml^{-1} control GNPs into the tail vein and sacrificed at the same time points as the first group. Their main organs (including liver, pancreas, brain, spleen, kidney and blood samples) were taken for analysis by Flame Atomic Absorption Spectroscopy (FAAS).

Rat experiment: 200 μl (30 mg ml^{-1}) of INS-GNPs were injected directly into the heart of a rat weighing 250 g. Three hours post-injection the rat was anesthetized and complete perfusion was performed. Then, the rat was sacrificed and the brain was extracted for CT scan and FAAS analysis.

Determination of the amount of GNPs across the BBB

Flame Atomic Absorption Spectroscopy (FAAA, SpectrAA 140, Agilent Technologies) was used to determine the amount of gold in the investigated samples. Samples were melted with aqua regia acid (a mixture of nitric acid and hydrochloric acid in a volume ratio of 1 : 3), filtered and diluted to a final volume of 10 ml. A calibration curve with known gold concentrations was prepared and the gold concentration was determined according to absorbance values, compared to calibration curves. All samples were analyzed by FAAS under the same experimental conditions.

In vivo CT experiments

Scans were performed using a micro-CT scanner (Skyscan High Resolution Model 1176), with the following scanning

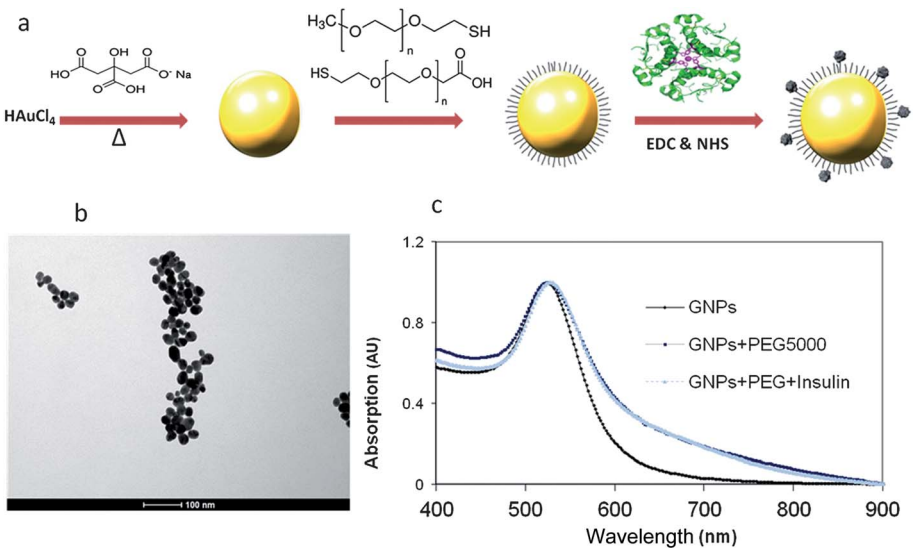

Fig. 2 Synthesis, functionalization and characterization of INS-GNPs. (a) Schematic diagram of the synthesis of 30 nm gold nanoparticles and functionalization with insulin. (b) TEM image of 20 nm GNPs (scale bar 100 nm). (c) Ultraviolet-visible spectroscopy of the bare GNPs, PEG coated GNPs and INS-GNPs.

parameters: tube voltage 50 kV_p, tube current 500 μA, 0.5 mm aluminum (Al) filtering and 18 μm (pixel size).

Results and discussion

Synthesis, conjugation and characterization of INS-GNPs

Transmission electron microscopy (TEM) showed that the GNPs were spheres, 20 nm in diameter, and uniformly distributed (Fig. 2b). INS-GNPs were characterized after each step of preparation using ultraviolet-visible spectroscopy (UV-1650 PC; Shimadzu Corporation, Kyoto, Japan). An expanded signal was observed following each layer of coating (Fig. 2c), confirming the chemical coating. Control nanoparticles were prepared by coating GNPs with a layer of mPEG-SH. This layer reduces nonspecific interactions and increases the blood circulation time of the nanoparticles, thereby making it an appropriate control to the INS-GNPs.[48,49] The chemical stability of the INS-GNP construct has been evaluated up to three months (using UV-Vis spectroscopy and TEM), and the particles were found to remain stable.

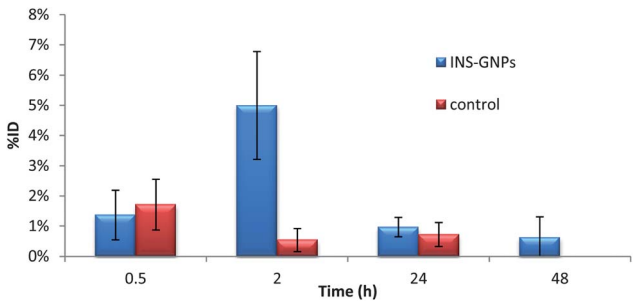

Fig. 3 Pharmacokinetics of INS-GNPs *vs.* control GNPs in the brain up to 48 h post-IV injection. 2 h post-injection, the amount of specifically targeted INS-GNPs found in mouse brains is over 5 times higher than that of the control, untargeted GNPs. Both the INS-GNPs and the control GNPs gradually cleared from the brain, so that only a negligible amount of INS-GNPs and no control GNPs were found in the brain 48 hours post-injection. Results are presented as percentage of the injected dose (%ID), mean ± S.D. *$P < 0.05$ statistical significance.

INS-GNPs across the BBB *in vivo*

To examine the quantity of INS-GNPs in the brain, as well as the whole body biodistribution, INS-GNPs and control GNPs were intravenously injected into the tail vein of male BALB/c mice. As demonstrated in Fig. 3, half an hour post-GNP injection, the quantity of INS-GNPs in the brain was similar to that of control GNPs. However, two hours post-injection a significant difference was observed – the amount of the specifically targeted INS-GNPs increased to 5 times greater than that of the control GNPs, demonstrating the effectiveness of the proposed method. Importantly, the pharmacokinetic results demonstrate that both the INS-GNPs and the control GNPs gradually cleared from the brain, so that only a negligible amount of INS-GNPs and no control GNPs were found in the brain 48 hours post-injection.

It is important to note that analysis of the entire brain for gold content includes the GNPs present in cerebral blood (which did not cross the BBB), as well as particles that actually crossed the BBB and accumulated in the brain. Therefore, in order to accurately calculate how many GNPs (amount of gold) penetrated the brain, the amount of gold in the cerebral blood was calculated and deducted from the total amount of gold found in the brain. The amount of gold in the cerebral blood was calculated by measuring the concentration of gold in the blood and multiplying by the cerebral blood volume, which is about 5.8% of the weight of the brain.[50] Fig. 4 compares the amount of gold found in the brain tissue (without cerebral blood) with that found in cerebral blood for both the INS-GNPs (a) and the control GNPs (b). These results clearly indicate that a significant quantity of INS-GNPs accumulated in the brain two hours post-injection and that this amount is much greater than that found in the cerebral blood. We hypothesize that the small amount of gold found in the brain at 24 and 48 hours post-injection, both for the INS-GNPs and the control GNPs, does not represent particles that penetrated the brain, but rather particles that were lodged in the blood vessels that form the BBB.

Fig. 5 presents the pharmacokinetics and biodistribution of INS-GNPs (a) and of the control group (b). As demonstrated, most of the particles accumulated in the liver and pancreas. Interestingly, results show significantly higher accumulation of

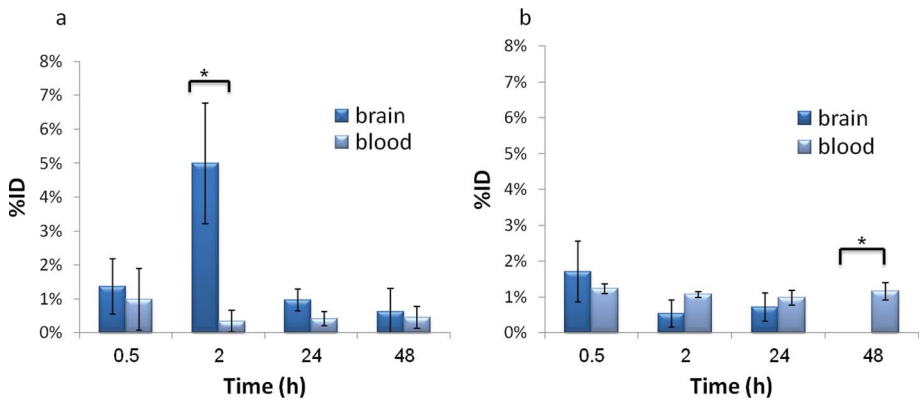

Fig. 4 Quantification of the amount of gold found in the brain tissue (without cerebral blood) and the amount of gold found in cerebral blood for the INS-GNPs (a) and the control GNPs (b). Results are presented as percentage of the injected dose (%ID), mean ± S.D. *$P < 0.05$ statistical significance with INS-GNPs in the brain *vs.* INS-GNPs in the blood.

(a)

%ID	0.5 h	2 h	24 h	48 h
Brain	1.37 ± 0.82	5 ± 1.78	0.97 ± 0.32	0.63 ± 0.68
Liver and Pancreas	49.07 ± 9.71	37.24 ± 10.26	52.26 ± 12.71	27.21 ± 14.9
Spleen	5.03 ± 1.36	4.53 ± 0.9	2.67 ± 0.7	4.83 ± 2.19
Kidney	15.97 ± 3.45	25.11 ± 4.58	16.97 ± 2.73	30.92 ± 5.84
Blood	26.64 ± 9.62	27.56 ± 15.5	26.61 ± 11.5	35.73 ± 16.66

(b)

%ID	0.5 h	2 h	24 h	48 h
Brain	1.71 ± 0.84	0.53 ± 0.38	0.72 ± 0.4	0
Liver and Pancreas	15.04 ± 4.17	17.61 ± 1.95	33.42 ± 5.33	23.15 ± 12.61
Spleen	3.13 ± 0.79	3.07 ± 0.45	4.88 ± 1.03	3.77 ± 0.08
Kidney	12.59 ± 3.04	13.5 ± 2.55	11.38 ± 4.41	13.24 ± 1.10
Blood	66.3 ± 6.83	64.22 ± 4.79	48.61 ± 8.19	59.47 ± 12.47

Fig. 5 Biodistribution and pharmacokinetics of INS-GNPs (top) and control GNPs (bottom) in mice. Results are given as mean ± S.D.

INS-GNPs in the liver and pancreas, in comparison with the control group at all time points (Fig. 6). This can be explained by the high expression of insulin receptors on the membrane of the pancreas and the liver,[51] which proves the specific interaction between insulin receptors and INS-GNPs, as well as the stability of the particles *in vivo*. In general, the nanoparticles accumulate in the kidney, liver, and spleen according to their well-described clearance mechanism.[52,53]

In order to verify the accumulation of INS-GNPs in the brain, an additional proof-of-principle experiment was performed on a rat model as described in the Experimental section under animal model and *in vivo* experiments. This time, in order to

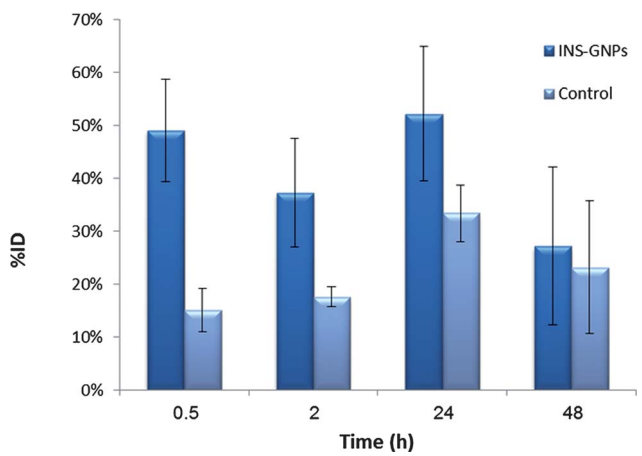

Fig. 6 Pharmacokinetics of INS-GNPs *vs.* control nanoparticles in the liver and pancreas. At all time points, higher accumulation of INS-GNPs compared to the control group has been observed. This can be explained by the high expression of insulin receptors on the membrane of the pancreas and the liver, which proves the specific interaction between insulin receptors and INS-GNPs. Results are presented as percentage of the injected dose (%ID), mean ± S.D.

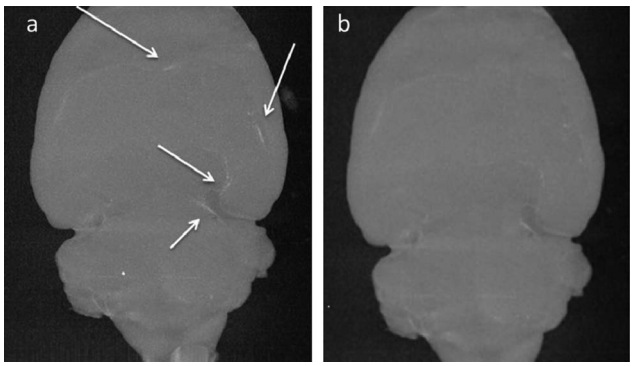

Fig. 7 A total intensity projection CT image of a rat brain after the perfusion process: (a) 3 h post-injection of INS-GNPs and (b) a control brain without GNPs. Specific brain regions with accumulation of INS-GNPs are marked by white arrows. Scanning parameters for the micro-CT (Skyscan High Resolution Model 1176) are 50 kV_p, 500 μA and 0.5 mm Al filtering.

eliminate the effect of cerebral intravascular GNPs, cerebral perfusion was performed. Fig. 7 presents a total intensity projection CT image of a rat brain after injection of INS-GNPs (a) and a control brain without GNPs (b). By comparing the two images, we can clearly identify specific brain regions with accumulation of INS-GNPs marked by white arrows. These bright areas can be differentiated from surrounding tissue, as gold induces stronger X-ray attenuation. A quantitative FAAS analysis confirmed CT results and found 0.0045 mg of gold in the rat brain, which is correlated with 0.64% of the injected dose. This perfusion experiment, which excluded the cerebral blood effect, provides further evidence that INS-GNPs crossed the BBB and accumulated in the brain.

The potential applicability of the proposed method strongly depends on the bio-safety of the GNPs. While almost any material can be toxic at a high enough dose, the more relevant question is: how toxic are gold nanoparticles at the potential relevant clinical concentrations. Throughout this research, the maximal injected dose was 6 mg per mouse, which has been proven to be non-toxic *in vivo*.[54,55] No acute toxicity was detected. All mice survived the full study period with no decline in well-being expressed by food intake, weight and normal behavior.

Conclusions

In summary, targeting insulin receptors has been found to be an effective approach, as the percentage of gold (5% from the total ID) that crossed the BBB and accumulated in the brain was found to be higher in comparison with other studies which investigated the penetration of various nanoparticle types into the brain (up to 0.5%).[56–58] This could be explained by the relatively small size of INS-GNPs, as well as by the effectiveness of insulin receptors in comparison with other receptors.[23] This study may have important implications in neurodegenerative diseases, since INS-GNPs could act as targeted drug delivery vehicles (the drug can be encapsulated by or attached to the particle) and increase the uptake of appropriate drugs in the

brain. This study suggests a new theranostic strategy for Alzheimer's disease: delivery of insulin to the brain could potentially serve both as an effective therapy to improve memory and as a diagnostic tool to identify Alzheimer's disease in its early stages, a tool which will make treatment more effective, hindering progression of the disease and its symptoms.

Conflict of interest disclosure

The authors have declared that no competing interest exists.

Acknowledgements

This work was supported by the Teva Pharmaceutical industries for their Network of Excellence in Neuroscience (NNE) doctoral scholarship and the Christians for Israel Chair in Medical Research. We thank Prof. Gal Yadid for stimulating discussions and feedback.

References

1 W. M. Pardridge, *Mol. Interventions*, 2003, **3**, 90–105, 151.
2 W. M. Pardridge, *NeuroRx*, 2005, **2**, 3–14.
3 I. van Rooy, S. Cakir-Tascioglu, W. E. Hennink, G. Storm, R. M. Schiffelers and E. Mastrobattista, *Pharm. Res.*, 2011, **28**, 456–471.
4 H. Davson and M. B. Segal, *Special aspects of the blood–brain barrier*, CRC Press, Boca Raton, 1996.
5 W. M. Pardridge and R. J. Boado, *Methods Enzymol.*, 2012, **503**, 269–292.
6 Y.-E. K. Lee and R. Kopelman, *Targeted, Multifunctional Hydrogel Nanoparticles for Imaging and Treatment of Cancer*, 2012.
7 C. Roney, P. Kulkarni, V. Arora, P. Antich, F. Bonte, A. M. Wu, N. N. Mallikarjuana, S. Manohar, H. F. Liang, A. R. Kulkarni, H. W. Sung, M. Sairam and T. M. Aminabhavi, *J. Controlled Release*, 2005, **108**, 193–214.
8 S. Bhaskar, F. R. Tian, T. Stoeger, W. Kreyling, J. M. de la Fuente, V. Grazu, P. Borm, G. Estrada, V. Ntziachristos and D. Razansky, *Part. Fibre Toxicol.*, 2010, **7**, 25.
9 N. Denora, A. Trapani, V. Laquintana, A. Lopedota and G. Trapani, *Curr. Top. Med. Chem.*, 2009, **9**, 182–196.
10 R. Arvizo, R. Bhattacharya and P. Mukherjee, *Expert Opin. Drug Delivery*, 2010, **7**, 753–763.
11 I. P. Kaur, R. Bhandari, S. Bhandari and V. Kakkar, *J. Controlled Release*, 2008, **127**, 97–109.
12 P. R. Lockman, R. J. Mumper, M. A. Khan and D. D. Allen, *Drug Dev. Ind. Pharm.*, 2002, **28**, 1–13.
13 R. Singh and J. W. Lillard, *Exp. Mol. Pathol.*, 2009, **86**, 215–223.
14 Y.-E. L. Koo, G. R. Reddy, M. Bhojani, R. Schneider, M. A. Philbert, A. Rehemtulla, B. D. Ross and R. Kopelman, *Adv. Drug Delivery Rev.*, 2006, **58**, 1556–1577.
15 D. A. Orringer, Y. E. Koo, T. Chen, R. Kopelman, O. Sagher and M. A. Philbert, *Clin. Pharmacol. Ther.*, 2009, **85**, 531–534.
16 R. Gabathuler, *Neurobiol. Dis.*, 2010, **37**, 48–57.
17 A. R. Jones and E. V. Shusta, *Pharm. Res.*, 2007, **24**, 1759–1771.
18 W. M. Pardridge, *J. NeuroVirol.*, 1999, **5**, 556–569.
19 S. C. Woods, R. J. Seeley, D. G. Baskin and M. W. Schwartz, *Curr. Pharm. Des.*, 2003, **9**, 795–800.
20 J. Kreuter, D. Shamenkov, V. Petrov, P. Ramge, K. Cychutek, C. Koch-Brandt and R. Alyautdin, *J. Drug Targeting*, 2002, **10**, 317–325.
21 B. Petri, A. Bootz, A. Khalansky, T. Hekmatara, R. Muller, R. Uhl, J. Kreuter and S. Gelperina, *J. Controlled Release*, 2007, **117**, 51–58.
22 K. Ulbrich, T. Hekmatara, E. Herbert and J. Kreuter, *Eur. J. Pharm. Biopharm.*, 2009, **71**, 251–256.
23 K. Ulbrich, T. Knobloch and J. Kreuter, *J. Drug Targeting*, 2011, **19**, 125–132.
24 L. A. Needleman and A. K. McAllister, *Neuron*, 2008, **58**, 653–655.
25 S. Craft, L. D. Baker, T. J. Montine, S. Minoshima, G. S. Watson, A. Claxton, M. Arbuckle, M. Callaghan, E. Tsai, S. R. Plymate, P. S. Green, J. Leverenz, D. Cross and B. Gerton, *Arch. Neurol.*, 2012, **69**, 29–38.
26 L. Frolich, D. Blum-Degen, H. G. Bernstein, S. Engelsberger, J. Humrich, S. Laufer, D. Muschner, A. Thalheimer, A. Turk, S. Hoyer, R. Zochling, K. W. Boissl, K. Jellinger and P. Riederer, *J. Neural Transm.*, 1998, **105**, 423–438.
27 H. Schiöth, S. Craft, S. Brooks, W. Frey and C. Benedict, *Mol. Neurobiol.*, 2011, 1–7.
28 C. Benedict, W. H. Frey, 2nd, H. B. Schioth, B. Schultes, J. Born and M. Hallschmid, *Exp. Gerontol.*, 2011, **46**, 112–115.
29 W. M. Pardridge, *Adv. Drug Delivery Rev.*, 2007, **59**, 141–152.
30 P. Ghosh, G. Han, M. De, C. K. Kim and V. M. Rotello, *Adv. Drug Delivery Rev.*, 2008, **60**, 1307–1315.
31 Z. Guodong, Y. Zhi, L. Wei, Z. Rui, H. Qian, T. Mei, L. Li, L. Dong and L. Chun, *Biomaterials*, 2009, **30**, 1928–1936.
32 C. Lasagna-Reeves, D. Gonzalez-Romero, M. A. Barria, I. Olmedo, A. Clos, V. M. S. Ramanujam, A. Urayama, L. Vergara, M. J. Kogan and C. Soto, *Biochem. Biophys. Res. Commun.*, 2010, **393**, 649–655.
33 S. K. Balasubramanian, J. Jittiwat, J. Manikandan, C. N. Ong, L. E. Yu and W. Y. Ong, *Biomaterials*, 2010, **31**, 2034–2042.
34 J. Lipka, M. Semmler-Behnke, R. A. Sperling, A. Wenk, S. Takenaka, C. Schleh, T. Kissel, W. J. Parak and W. G. Kreyline, *Biomaterials*, 2010, **31**, 6574–6581.
35 N. Chanda, V. Kattumuri, R. Shukla, A. Zambre, K. Katti, A. Upendran, R. R. Kulkarni, P. Kan, G. M. Fent, S. W. Casteel, C. J. Smith, E. Boote, J. D. Robertson, C. Cutler, J. R. Lever, K. V. Katti and R. Kannan, *Proc. Natl. Acad. Sci. U. S. A.*, 2010, **107**, 8760–8765.
36 A. Kunzmann, B. Andersson, T. Thurnherr, H. Krug, A. Scheynius and B. Fadeel, *Biochim. Biophys. Acta, Gen. Subj.*, 2011, **1810**, 361–373.
37 I. H. El-Sayed, *Curr. Oncol. Rep.*, 2010, **12**, 121–128.
38 H. J. Johnston, G. Hutchison, F. M. Christensen, S. Peters, S. Hankin and V. Stone, *Crit. Rev. Toxicol.*, 2010, **40**, 328–346.
39 C. M. Cobley, L. Au, J. Y. Chen and Y. N. Xia, *Expert Opin. Drug Delivery*, 2010, **7**, 577–587.

40 X. D. Zhang, H. Y. Wu, D. Wu, Y. Y. Wang, J. H. Chang, Z. B. Zhai, A. M. Meng, P. X. Liu, L. A. Zhang and F. Y. Fan, *Int. J. Nanomed.*, 2010, **5**, 771–781.
41 R. Ankri, H. Duadi, M. Motiei and D. Fixler, *J. Biophotonics*, 2012, **5**, 263–273.
42 R. Ankri, V. Peretz, M. Motiei, R. Popovtzer and D. Fixler, *Int. J. Nanomed.*, 2012, **7**, 449–455.
43 E. E. Connor, J. Mwamuka, A. Gole, C. J. Murphy and M. D. Wyatt, *Small*, 2005, **1**, 325–327.
44 T. Reuveni, M. Motiei, Z. Romman, A. Popovtzer and R. Popovtzer, *Int. J. Nanomed.*, 2011, **6**, 2859–2864.
45 A. I. Sherman and M. Ter-Pogossian, *Cancer*, 1953, **6**, 1238–1240.
46 M. Shilo, T. Reuveni, M. Motiei and R. Popovtzer, *Nanomedicine*, 2012, **7**, 257–269.
47 B. V. Enustun and J. Turkevich, *J. Am. Chem. Soc.*, 1963, **85**, 3317–3328.
48 S. M. Moghimi, A. C. Hunter and J. C. Murray, *Pharmacol. Rev.*, 2001, **53**, 283–318.
49 R. Gref, M. Luck, P. Quellec, M. Marchand, E. Dellacherie, S. Harnisch, T. Blunk and R. H. Muller, *Colloids Surf., B*, 2000, **18**, 301–313.
50 B. P. Chugh, J. P. Lerch, L. X. Yu, M. Pienkowski, R. V. Harrison, R. M. Henkelman and J. G. Sled, *NeuroImage*, 2009, **47**, 1312–1318.
51 M. Korc, H. Sankaran, K. Y. Wong, J. A. Williams and I. D. Goldfine, *Biochem. Biophys. Res. Commun.*, 1978, **84**, 293–299.
52 S. D. Li and L. Huang, *Mol. Pharm.*, 2008, **5**, 496–504.
53 J. P. M. Almeida, A. L. Chen, A. Foster and R. Drezek, *Nanomedicine*, 2011, **6**, 815–835.
54 J. F. Hainfeld, M. J. O'Connor, F. A. Dilmanian, D. N. Slatkin, D. J. Adams and H. M. Smilowitz, *Br. J. Radiol.*, 2011, **84**, 526–533.
55 J. F. Hainfeld, D. N. Slatkin, T. M. Focella and H. M. Smilowitz, *Br. J. Radiol.*, 2006, **79**, 248–253.
56 P. R. Lockman, M. O. Oyewumi, J. M. Koziara, K. E. Roder, R. J. Mumper and D. D. Allen, *J. Controlled Release*, 2003, **93**, 271–282.
57 E. Afergan, H. Epstein, R. Dahan, N. Koroukhov, K. Rohekar, H. D. Danenberg and G. Golomb, *J. Controlled Release*, 2008, **132**, 84–90.
58 Y. Xie, L. Y. Ye, X. B. Zhang, W. Cui, J. N. Lou, T. Nagai and X. P. Hou, *J. Controlled Release*, 2005, **105**, 106–119.